The Journal of Immunology

Free Ig Light Chains Interact with Sphingomyelin and Are Found on the Surface of Myeloma Plasma Cells in an Aggregated Form

Andrew T. Hutchinson, Paul A. Ramsland, Darren R. Jones, Mark Agostino, Maria E. Lund, Cameron V. Jennings, Vanessa Bockhorni, Elizabeth Yuriev, Allen B. Edmundson and Robert L. Raison

J. Immunol. 2010;185;4179-4188; originally published online Sep 3, 2010;
doi:10.4049/jimmunol.1001956
http://www.jimmunol.org/cgi/content/full/185/7/4179

The Journal of Immunology is published twice each month by The American Association of Immunologists, Inc., 9650 Rockville Pike, Bethesda, MD 20814-3994.

Print ISSN: 0022-1767 Online ISSN: 1550-6606.

Free Ig Light Chains Interact with Sphingomyelin and Are Found on the Surface of Myeloma Plasma Cells in an Aggregated Form

Andrew T. Hutchinson,* Paul A. Ramsland,[†,‡,§] Darren R. Jones,* Mark Agostino,[¶] Maria E. Lund,* Cameron V. Jennings,* Vanessa Bockhorni,* Elizabeth Yuriev,[¶] Allen B. Edmundson,[‖] and Robert L. Raison*

Free κ L chains (FκLCs) are expressed on the surface of myeloma cells and are being assessed as a therapeutic target for the treatment of multiple myeloma. Despite its clinical potential, the mechanism by which FκLCs interact with membranes remains unresolved. In this study, we show that FκLCs associate with sphingomyelin on the plasma membrane of myeloma cells. Moreover, membrane-bound FκLCs are aggregated, suggesting that aggregation is required for intercalation with membranes. Finally, we propose a model where the binding of FκLCs with sphingomyelin on secretory vesicle membranes is stabilized by self-aggregation, with aggregated FκLCs exposed on the plasma membrane after exocytosis. Although it is well known that protein aggregates bind membranes, this is only the second example of an aggregate being found on the surface of cells that also secrete the protein in its native form. We postulate that many other aggregation-prone proteins may associate with cell membranes by similar mechanisms. ***The Journal of Immunology*****, 2010, 185: 4179–4188.**

Multiple myeloma (MM) is characterized by the uncontrolled proliferation of plasma cells and the accumulation of their secreted monoclonal free Ig L chain (FLC) (1). A complication frequently observed in MM patients is the deposition of FLC aggregates in organs. These can be as ordered amyloid fibrils (referred to as LC amyloidosis), or amorphous deposits (LC deposition disease). The formation of LC aggregates is thought to be due to partial unfolding of FLCs into an intermediate structure and subsequent self-association of adjacent β strands (2–5). Protein denaturation methods, such as heat and high-ionic strength buffers, can promote FLC aggregation in vitro (3, 6). Very little is known about the process in vivo, although a recent study suggested that FLC aggregation can be induced by interactions with biological membranes (7).

There are two isotypes of FLCs, designated κ or λ, with the former accounting for 61% of MM cases (8). The mAb K-1-21 recognizes a conformational epitope on free κ LCs (FκLCs) (9). Interestingly, it also binds a cell surface-associated form of FκLC, termed κ myeloma Ag (KMA), expressed on plasma cells from patients with κLC isotype MM and on malignant cells in other B cell lineage diseases such as Waldenström's macroglobulinemia and non-Hodgkin's lymphoma (10–12). The expression of KMA on a range of B cell malignancies has led to the development of a human chimeric IgG1 version of K-1-21, designated MDX1097, which has recently undergone a phase I clinical trial for the treatment of κLC isotype MM (13).

The mechanism by which FκLCs associate with the cell membrane to form KMA is not immediately clear given the absence of recognizable structural motifs through which they may intercalate in the lipid bilayer. Early immunoprecipitation attempts on KMA-expressing cells by K-1-21 revealed that the Ag is primarily composed of FκLCs. In the same study, actin was identified as a protein that coprecipitated with KMA and hence may have played a role in the association of FκLCs with the cell membrane (14). However, subsequent immunoprecipitation attempts have failed to identify actin or any proteins other than FκLCs in the KMA complex (Supplemental Fig. 1). Given the potential of KMA as a therapeutic target, the mode by which FκLCs could be bound to the plasma membrane remains of considerable interest.

In this study, we show that KMA consists of only FκLCs in direct association with the plasma membrane of FκLC-secreting cells. Molecular characterization of KMA reveals that FκLCs are in an aggregated form, which suggests that this is a requirement for stable association with membranes. Furthermore, binding studies using large unilamellar vesicles (LUVs) show that FκLCs associate with membranes composed of saturated phosphocholine (PC) lipids such as sphingomyelin. This was confirmed in FκLC-

*Department of Medical and Molecular Biosciences, University of Technology Sydney, Ultimo, New South Wales; [†]Centre for Immunology, Burnet Institute; [‡]Department of Surgery, Austin Health, University of Melbourne, Heidelberg; [§]Department of Immunology, Monash University, Alfred Medical Research and Education Precinct, Melbourne; [¶]Medicinal Chemistry and Drug Action, Monash Institute of Pharmaceutical Sciences, Monash University, Parkville, Victoria, Australia; and [‖]Protein Crystallography Program, Oklahoma Medical Research Foundation, Oklahoma City, OK 73104

Received for publication June 14, 2010. Accepted for publication August 2, 2010.

This work was supported by Immune System Therapeutics Ltd, Australia. M.A. is a recipient of an Australian Postgraduate Award. P.A.R. is a recipient of an R. Douglas Wright Career Development Award (ID365209) from the National Health and Medical Research Council of Australia. This work was also supported by the Victorian Operational Infrastructure Support Program (to the Burnett Institute).

Address correspondence and reprint requests to Dr. Andrew Hutchinson, Department of Medical and Molecular Biosciences, University of Technology Sydney, PO Box 123, Ultimo, NSW 2007, Australia. E-mail address: andrew.hutchinson@uts.edu.au

The online version of this article contains supplemental material.

Abbreviations used in this paper: AP, alkaline phosphatase; BN, blue native; CL, constant L chain domain; D_H, hydrodynamic diameter; DLS, dynamic light scattering; DOPC, 1,2-dioleoyl-*sn*-glycero-3-phosphatidylcholine; ER, endoplasmic reticulum; FκLC, free κ L chain; FLC, free L chain; HC, H chain; KMA, κ myeloma Ag; LC, L chain; LUV, large unilamellar vesicle; MM, multiple myeloma; PC, phosphocholine; POPC, 1-palmitoyl-2-oleoyl-*sn*-glycero-3-phosphatidylcholine; POPE, 1-palmitoyl-2-oleoyl-*sn*-glycero-3-phosphatidylethanolamine; POPS, 1-palmitoyl-2-oleoyl-*sn*-glycerol-3-phosphatidylserine; RU, arbitrary response unit; SPR, surface plasmon resonance; TX100, Triton X-100; VL, variable L chain domain.

secreting cell lines in which blockage of the breakdown of sphingomyelin resulted in increased levels of sphingomyelin and concomitant KMA expression. Collectively, the results support a model for KMA expression by B cells where FκLCs interact with sphingomyelin and undergo aggregation leading to stable association with membranes in secretory vesicles destined for exocytosis. It follows that fusion of the vesicle with the plasma membrane exposes membrane-associated FκLCs on the extracellular face of the cell as KMA. Although a large number of protein aggregates have been shown to bind membranes (reviewed in Ref. 15), this is only the second time protein aggregates have been observed on the surface of cells secreting a protein in its native form (16). Based on these findings, we postulate that many other aggregation-prone proteins may associate with plasma membranes of secretory cells by similar mechanisms.

Materials and Methods

Cell lines and general reagents

ARH-77_100 (ATCC No. CRL-1621) and NCI-H929 (ATCC No. CRL-9068) cell lines were obtained from the American Type Culture Collection (Manassas, VA). ARH-77_neg (DSMZ No. ACC-512) and JJN-3 (DSMZ No. ACC-541) cell lines were obtained from the German Resource Center for Biological Material (DSMZ; Braunschweig, Germany). The HEK-293 cell line was obtained from Invitrogen (Rowville, Victoria, Australia). Cell lines were cultured according to recommendations from the supplier.

K-1-21 was produced commercially by the Australian Commonwealth Scientific and Research Organization (Clayton South,Victoria, Australia). MDX1097 was produced by Medarex (Princeton, NJ). Batches of MDX1097 and human IgG isotype control (Sigma-Aldrich, Castle Hill, New South Wales, Australia) were labeled with allophycocyanin by Invitrogen.

FκLCs were purified from the urine of MM patients by ammonium sulfate precipitation as described previously (9). Lysenin and BSA were obtained from Sigma-Aldrich.

Flow cytometry

Cells were stained with MDX1097-allophycocyanin (or human IgG-allophycocyanin) for detection of KMA. For sphingomyelin detection, cells were incubated with 5 μg/ml biotinylated lysenin for 30 min on ice followed by streptavidin-allophycocyanin. Fluorescence was recorded on a FACSCalibur flow cytometer (BD Biosciences, North Ryde, New South Wales, Australia) and then analyzed by FCS Express V3 software (De Novo Software, Los Angeles, CA).

In the experiments indicated, cells were incubated with 5 μM GW4869 (Sigma-Aldrich) under normal tissue culture conditions. After 48 h, cells were harvested for downstream flow cytometric analysis.

Measurement of FκLC secretion

ARH-77_100, ARH-77_neg, NCI-H929, and JJN-3 cells were set up at 2×10^5 cells/ml and incubated at cell culture conditions for 96 h. Supernatants were kept then assessed for FκLC secretion by K-1-21 ELISA. Briefly, ELISA plates were precoated with K-1-21 and then samples were added to each well in triplicate. Plates were incubated for 90 min at 37°C. Bound FκLCs were detected with anti-κLC alkaline phosphatase (AP) (Sigma-Aldrich).

Sodium carbonate membrane extraction

Cellular membranes were prepared from ARH-77_100 or JJN-3 cells according to previously described methods (17). The following membrane extraction method is adapted from Fujiki et al. (18). Membranes were treated with 0.1 M Na_2CO_3 at pH 11 for 30 min on ice, followed by centrifugation at 20,000 × *g* for 30 min. Membranes were washed in PBS/sodium azide twice and then pelleted at 20,000 × *g*. Membranes were resuspended in 1% (v/v) Triton X-100 (TX100) PBS/sodium azide and centrifuged to remove cell debris.

Samples were separated by SDS-PAGE under nonreducing conditions followed by transfer to nitrocellulose membranes and Western blotting with rabbit anti-actin (Sigma-Aldrich) and rabbit anti-calnexin (Sigma-Aldrich) with the secondary Ab being anti-rabbit IgG peroxidase (Sigma-Aldrich). The κLC was detected by a goat anti-human κLC AP-conjugated IgG (Sigma-Aldrich).

Two-dimensional blue native and SDS-PAGE

Blue native (BN)-PAGE was performed using 4–16% native PAGE precast gels by the procedure described by the manufacturer for BN-PAGE analysis (Invitrogen). When performing second dimension SDS-PAGE on BN-PAGE–fractionated samples, the lane of interest was equilibrated in SDS-loading buffer then separated in a 4–12% Bis-Tris gel (Invitrogen) followed by Western blotting with anti-κLC AP.

Dynamic light scattering measurements of FκLC

Dynamic light scattering (DLS) measurements were made on a Zetasizer Nano ZS instrument (Malvern, U.K.) fitted with a 633-nm helium-neon laser. To assess the point at which FκLCs began to form aggregates, a temperature analysis was performed whereby readings were made from 25°C to 65°C. Additionally, readings were made at 37°C and 50°C as well as at 37°C after 15 min of incubation at 50°C. Data were analyzed by Dispersion Technology Software from Malvern Instruments (Sutherland, New South Wales, Australia). The hydrodynamic diameter (D_H) was determined by the cumulants method (19). Percentage intensity versus particle size was determined by nonlinear least squares analysis of the DLS correlation functions.

Preparation of LUVs

LUVs were made according to the method described by Hope et al. (20). Phospholipids (20 mg) were dissolved in 2 ml of chloroform. Additionally, 4 μl of the pink lipophilic tracer dye 1,1′-dioctadecyl-3,3,3′,3′-tetramethylindocarbocyanine perchlorate (Invitrogen) was added so that LUVs could be visualized later. The lipid mixture was placed into a round-bottom glass flask, and chloroform was removed by rotary evaporation and then lyophilized overnight. Lipids were hydrated in 2 ml of PBS with 10% sucrose. The mixture was placed onto a mini-extruder (Avanti Polar Lipids, Alabaster, AL) and passed through a 100-nm polycarbonate filter to generate LUVs.

FκLC-LUV sucrose flotation assay

LUVs (250 μl) were incubated with 1 mg/ml FκLCs for the times and temperatures indicated. The LUV-FκLC mixture was transferred to a centrifuge tube and overlaid with a discontinuous sucrose gradient in PBS/sodium azide containing 3 ml of 60%, 4 ml of 40%, 3 ml of 20%, and 2 ml of 5% sucrose. The sample was then centrifuged at 100,000 × *g* for 20 h. Samples (1 ml) were taken from the top, with fraction No. 3 representing the LUV fraction. Fraction No. 10 consisted of the bottom 3 ml.

For densitometry, each fraction was separated by reducing SDS-PAGE and then developed by silver stain. The gels were photographed with a ChemiDoc imager (Bio-Rad Laboratories, Gladesville, New South Wales, Australia), and the average density of bands was assessed by Quantity One 1-D analysis software (Bio-Rad Laboratories). The density of each lane was expressed relative to the density of the bottom fraction.

Surface plasmon resonance (SPR) was performed on a Biacore 2000 (GE Healthcare, Rydalmere, New South Wales, Australia). Fraction No. 3 from each sample and FκLC-positive controls were injected at a flow rate of 20 μl/min for 5 min over an MDX1097-coated CM5 sensor chip (GE Healthcare). Arbitrary response units (RUs) were measured 2.5 min after the injection.

Phospholipid ELISA

PolySorp 96-well ELISA plates (Nunc, Roskilde, Denmark) were dried under nitrogen gas with 100 μl of 100 μg/ml lipids dissolved in ethanol. Wells were washed with 200 μl of 0.3% BSA-PBS and then blocked with 100 μl of 1% BSA-PBS for 1 h at 37°C. Aliquots (100 μl) of either 200 μg/ml biotinylated FκLCs or human κ Fab (purchased from Bethyl Laboratories, Montgomery, TX) were added to the wells, performing serial dilutions in 0.3% BSA-PBS. Plates were incubated for 90 min at 37°C, and then bound protein was detected by ExtrAvidin AP. Phospholipids were purchased from Avanti Polar Lipids.

Sphingomyelin assay

Determination of cellular sphingomyelin content was performed as previously described by Hojjati and Jiang (21). Additionally, a BCA protein assay was performed on the samples according to the manufacturer's recommendations (Thermo Scientific, Rockford, IL). Total cellular sphingomyelin was calculated with reference to the standard curve and was expressed as either per 10^7 cells or per milligram of protein.

Transfection of κLCs into HEK-293 cells

Expression plasmids (pT-Rex) encoding full-length JJN-3 κLCs and constant domain only κLCs (starting at Val^{104}) were transfected into HEK-293 cells by the FreeStyle Max expression system (Invitrogen). Three days after transfection, cells were harvested and analyzed for KMA expression

by flow cytometry. Supernatants were also assessed for FκLC secretion levels by MDX1097 SPR.

Molecular modeling of PC-FκLC complexes

All modeling programs used in this study are from Schrödinger (New York, NY). Coordinates for PC were extracted from the Protein Data Bank (PDB) entry 2MCP and parameterized using the OPLS force field using MacroModel version 9.7. PC was docked in its zwitterionic form. The crystal structure of DEL (PDB code 1B6D), a noncovalent human κLC dimer (22), was prepared using the Protein Preparation Wizard in Maestro, version 9.0. Molecular docking was performed using Extra Precision (XP) mode in Glide, version 5.5 (Schrödinger). The scoring grids were set up within a cubic box (30 Å sides) centered at the centroid of the following residues: Gln^{37}, Lys^{39}, Lys^{45}, Leu^{47}, Pro^{59}, Arg^{61}, Phe^{62}, Glu^{81}, Asp^{82}. Grids were generated for each of the two sites of the dimer. Docked poses were clustered to a root mean square deviation of 2.0 Å. All other program settings were kept to defaults.

Results

Expression of KMA is not directly related to the level of FκLC secretion in MM cell lines

Four κLC isotype MM-derived cell lines, JJN-3, NCI-H929, ARH-77_100, and ARH-77_neg, were assessed for KMA expression by immunostaining with MDX1097 and analysis by flow cytometry. KMA was detected on JJN-3 and ARH-77_100 cells but was not expressed on NCI-H929 and ARH-77_neg cells (Fig. 1*A*). To verify that these cell lines were secreting FκLCs, day 4 cell culture supernatants were assessed for the presence of FκLCs by ELISA (Fig. 1*B*). To allow comparisons between cell lines, the amount of secreted FκLCs was normalized to final cell density. As expected, all cell lines secreted FκLCs, although the amounts varied widely between cell lines. Interestingly, the highest FκLC secretor was the non-KMA–expressing cell line NCI-H929 (5.71 ± 0.33 pg/cell). JJN-3 cells secreted intermediate levels of FκLCs and strongly expressed KMA (1.63 ± 0.05 pg/cell). Furthermore, whereas ARH-77_100 (0.29 ± 0.02 pg/cell) and ARH-77_neg (0.29 ± 0.03 pg/cell) secreted equivalent, yet small amounts of FκLCs, only ARH-77_100 expressed KMA (Fig. 1). This infers that there are additional factors involved in KMA expression by plasma cells other than the synthesis of FκLCs alone.

KMA consists of a high-molecular mass complex of FκLCs associated with the membrane via electrostatic and hydrophobic interactions

The molecular nature of KMA was investigated by analysis of plasma membrane proteins using BN-PAGE. Plasma membranes from KMA-expressing ARH-77_100 cells were fractionated by BN-PAGE followed by Western blotting for κLCs. The κLCs in the ARH-77_100 membrane fraction was present in a complex of ~480 kDa. In contrast, when soluble FκLCs were subjected to electrophoresis under the same conditions, they were found to migrate with a relative molecular mass of ~66 kDa, which is the approximate size of a FκLC dimer (Fig. 2*A*). This finding suggests that KMA consists of FκLCs that reside in a membrane-associated high-molecular mass complex. To exclude the possibility that this complex may contain H chain (HC)-associated κLCs in the form of intact Ig, ARH-77_100 membrane proteins fractionated by BN-PAGE in the first dimension were then subjected to SDS-PAGE under nonreducing conditions in the second dimension. κLCs, detected by Western blot, migrated at an approximate molecular mass of 28 kDa, thus confirming the presence of FκLCs in the 480 kDa complex (Fig. 2*B*). Furthermore, the failure to detect components in the molecular mass range >98 kDa in the SDS-PAGE dimension confirmed that HC-associated κLCs in the form of intact Ig was not present in the 480 kDa complex. In contrast to immunoprecipitation experiments where covalent FκLC dimers are often observed (Supplemental Fig. 1), covalent dimers were not present in the BN-PAGE/SDS-PAGE fractionated material. We have noted that when membranes are solubilized in the presence of an alkylating agent, covalent dimers are not found (Supplemental Fig. 2), leading to the conclusion that the formation of covalent dimers is a postsolubilization oxidation effect and does not occur under the conditions used for BN-PAGE.

Despite one early report that identified actin as a KMA-associated protein in immunoprecipitates (14), we have consistently failed to identify any non-FκLC components in immunoprecipitates of KMA (Supplemental Fig. 1). This suggests that FκLC associates directly with the plasma membrane to form KMA rather than being bound to a membrane-associated receptor. A simple method to determine the mode of interaction of a protein with membranes is to incubate them with high-ionic strength, high-pH Na_2CO_3 buffer. If the membrane protein is associated primarily through electrostatic forces, which are typical of both receptor–ligand interactions and peripheral membrane proteins, then the complexes are easily disrupted and dissociated from the membrane. If, however, the protein is integral and primarily associates with the membrane through hydrophobic interactions with the acyl core of the lipid bilayer, then it will be highly resilient to such treatments (18, 23).

Purified membranes from ARH-77_100 and JJN-3 were incubated with 0.1 M Na_2CO_3 (pH 11) buffer for 30 min. After incubation, membranes were pelleted by centrifugation and supernatant was collected for analysis of proteins that were released following disruption of electrostatic interactions. Treated membranes were then washed three times in PBS and solubilized in

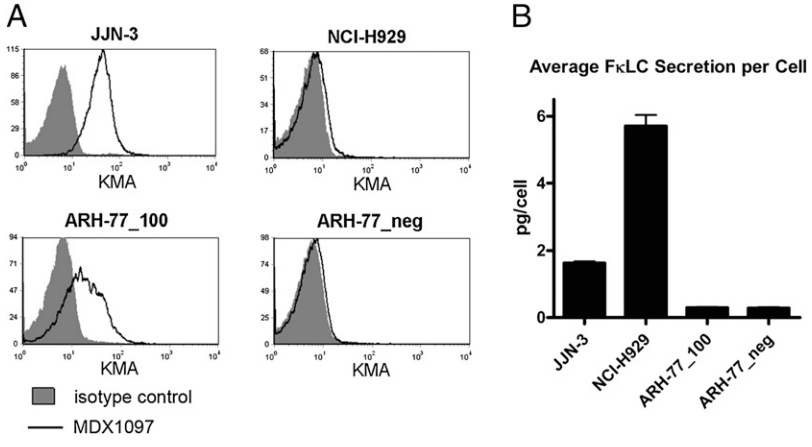

FIGURE 1. KMA expression does not correlate with the level of FκLC secretion. *A*, FACS analysis of MM-derived κLC cell lines stained with MDX1097-allophycocyanin (black histograms) or human IgG-allophycocyanin control (gray histograms). *B*, Total FκLC secretion measured by K-1-21–specific ELISA and expressed relative to final cell density. Data presented are means ± SE from three measurements (except NCI-H929, which is from two measurements).

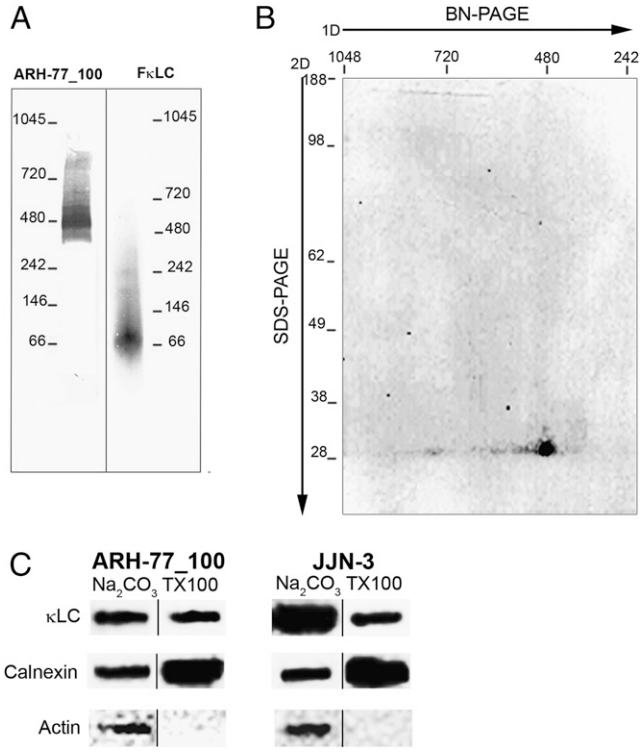

FIGURE 2. Membrane-associated FκLC, as KMA, resides in a large molecular complex and is directly associated with the cell membrane. *A*, ARH-77_100 membrane proteins and soluble FκLCs were separated by BN-PAGE and then Western blotted to detect κLCs. *B*, ARH-77_100 membrane proteins were separated by BN-PAGE then subjected to nonreducing SDS-PAGE in the second dimension followed by Western blotting to detect κLCs. *C*, Cell membranes from KMA expressing cell lines were solubilized with either Na_2CO_3 or TX100 and the extracts subjected to SDS-PAGE. Western blots were probed with Abs specific for κLCs, calnexin, or actin.

1% TX100. This was followed by one round of centrifugation to remove TX100-insoluble proteins. The Na_2CO_3 and TX100-soluble fractions were fractionated by SDS-PAGE and assessed by Western blot probing for κLCs. As controls, calnexin and actin, being integral and peripheral membrane proteins, respectively (24, 25), were detected by Western blot.

As expected, the peripheral membrane protein actin was only recovered in the Na_2CO_3 aqueous fraction. Calnexin, being a typical integral membrane protein, was found predominantly in the TX100 detergent fraction, with a small amount recovered in the Na_2CO_3 aqueous fraction (Fig. 2*C*). Although it was surprising to see some calnexin recovered in the Na_2CO_3 fraction, this result is in line with a previous report that showed that calnexin can be released from membranes by Na_2CO_3 extraction (26).

Interestingly, FκLC was recovered in both fractions. For ARH-77_100 membranes, FκLC was equally distributed across the aqueous and detergent fractions, whereas for JJN-3 membranes, FκLC was found predominantly in the Na_2CO_3 aqueous fraction, with ~25% being present in the TX100 fraction (Fig. 2*C*). Based on these results, membrane-associated FκLCs appear to be more resistant to Na_2CO_3 treatment than to actin, but less so than to calnexin. We interpret these findings as indicating that there are both electrostatic and hydrophobic interactions involved in the association of FκLCs with the cell membrane. Based on these results, KMA cannot be clearly designated as either a peripheral or an integral membrane protein. Interestingly, extraction of membranes with TX114 or urea show that FκLC behaves more like calnexin than actin in its ability to associate with membranes (Supplemental Fig. 3), which reinforces the conclusion that KMA cannot be classed as a typical peripheral membrane protein where electrostatic forces are the dominant mode of attachment.

Aggregated FκLCs bind membranes

The finding that KMA consists of a high-molecular mass complex containing FκLCs that are directly associated with the plasma membrane raised the possibility that the FκLCs in KMA are in an aggregated form.

To assess whether FκLC aggregation is required for membrane association, we initially determined the temperature at which FκLCs assembled into aggregates by DLS measurements. At temperatures >49°C, the D_H of FκLCs was seen to increase markedly (Fig. 3*A*), and this was interpreted as the temperature at which FκLCs began to assemble into aggregates. Additionally, we compared the size distributions of FκLCs at 37°C and after 15 min of incubation at 50°C. There was a uniform increase in size distribution from a peak of 8 nm at 37°C to 21 nm at 50°C, indicating that aggregates had formed. After cooling samples back to 37°C, the FκLC aggregates remained at the same size, indicating that heat-induced aggregation is irreversible (Fig. 3*B*). These stable and soluble FκLC aggregates (solutions remained transparent) approximate the sizes of polymeric IgM, which have D_H of 34–37 nm when measured by DLS (27).

To determine whether the aggregation of FκLCs may play a role in the binding of the protein to membranes, studies were undertaken using LUVs as model membranes. LUVs were incubated with FκLCs for 15 min at either 37°C or 50°C to induce protein aggregation. The amount of FκLCs bound to LUVs was then assessed by isolating LUV-bound FκLCs by sucrose density gradient centrifugation. Fractions from the density gradient were subjected to SDS-PAGE followed by silver staining to reveal proteins. Densitometry of the silver-stained SDS-PAGE gels revealed that there was significant binding of FκLCs to LUVs when heated to 50°C as shown by a sharp peak in protein concentration at fraction No. 3, the fraction in which LUVs were found after centrifugation. However, when FκLCs were incubated with LUVs at 37°C, the protein was broadly distributed across fraction Nos. 3–10, whereas without LUVs the FκLC was only found in fraction Nos. 6–10, with the majority in Nos. 9 and 10 (Fig. 3*D*). Furthermore, these results were confirmed by SPR binding analysis of the density gradient fractions using an MDX1097-coated sensor chip that revealed the presence of FκLCs in fraction No. 3 for the sample heated to 50°C (804.2 ± 18.2 RUs) when compared with the sample incubated at 37°C (169.8 ± 5.8 RUs) and the no LUV control sample (no detectable binding) (Fig. 3*E*). Because heating induces aggregation and enhances FκLC membrane association, these data clearly support the hypothesis that KMA consists of membrane-associated aggregated FκLCs.

FκLCs associate with saturated PC lipids

Although the previous findings suggest that FκLCs require aggregation to associate with membranes as KMA, they do not explain why some, but not all, FκLC-secreting B cells express KMA. There is mounting evidence that phospholipids can promote aggregation of proteins and that the aggregation is determined mainly by the class of phospholipid species (reviewed in Ref. 15). Therefore, FκLCs may show a tendency to associate with a particular class of membrane lipid, suggesting that certain lipids could be more abundant in KMA-positive cells compared with KMA-negative cells.

Common species of phospholipids, namely sphingomyelin, 1-palmitoyl-2-oleoyl-*sn*-glycero-3-phosphatidylcholine (POPC), 1,2-dioleoyl-*sn*-glycero-3-phosphatidylcholine (DOPC), 1-palmitoyl-2-

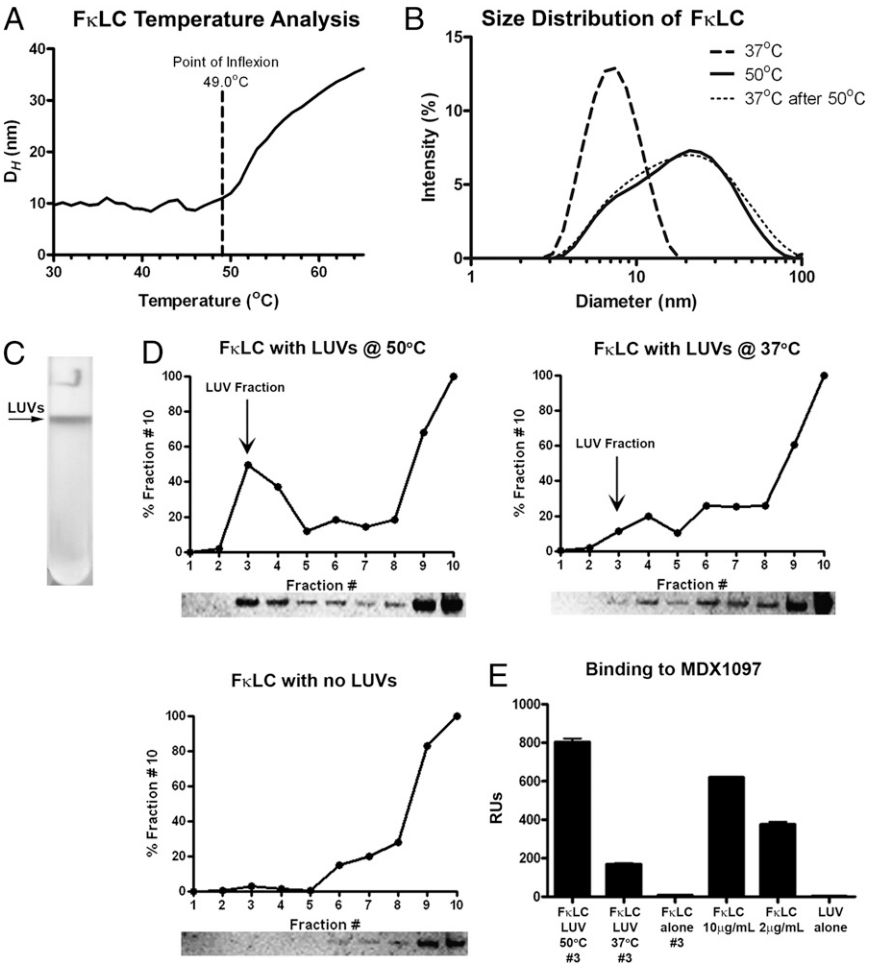

FIGURE 3. Heat-aggregated FκLCs bind to LUVs and are recognizable as KMA. *A*, DLS measurements of FκLCs at 1˚C increments over the temperature range 25–65˚C. *B*, Hydrodynamic diameter of FκLCs after heating for 15 min at 37˚C or 50˚C. Additionally, FκLCs heated at 50˚C were reassessed after cooling to 37˚C. *C–E*, LUVs were prepared in 10% sucrose and then incubated with FκLCs for 15 min at 37˚C or 50˚C to promote aggregation. The mixture was then centrifuged in a sucrose gradient to separate unbound FκLCs from LUVs. *C*, Photograph showing position of LUVs after centrifugation. The band, representing LUVs, is seen at the 5–20% sucrose interphase. *D*, SDS-PAGE of sucrose density fractions collected after centrifugation. Proteins were visualized by silver staining and subjected to densitometric analysis. Fractions are numbered from the top of the density gradient. *E*, SPR analysis of binding of MDX1097 to density gradient fraction No. 3 (LUV fraction). Binding of FκLCs at 2 and 10 μg/ml is included as control. Data presented are means ± SE from two measurements.

oleoyl-*sn*-glycero-3-phosphatidylethanolamine (POPE), and 1-palmitoyl-2-oleoyl-*sn*-glycerol-3-phosphatidylserine (POPS), were coated onto hydrophobic 96-well plates. These were dried under a stream of nitrogen, resulting in lipid monolayers. Plates were blocked with BSA and incubated with serial dilutions of biotinylated FκLCs or biotinylated Fab as a control. Bound protein was detected with streptavidin-AP conjugate. The highest level of binding by FκLCs was to sphingomyelin, followed by POPC, and the binding reached saturation at 100 μg/ml on both phospholipid monolayers. There was weaker binding to DOPC and POPS, while POPE showed no reactivity with FκLCs (Fig. 4*A*). Biotinylated Fab showed no binding at any of the concentrations tested (Fig. 4*B*).

Sphingomyelin, POPC, and DOPC represent disaturated, monosaturated, and unsaturated PC lipids, respectively. However, only sphingomyelin and POPC show association with FκLCs. This suggests a requirement for both a PC head group and saturated acyl tails to bind FκLCs. To confirm that FκLCs bind preferentially to saturated PC-type lipids, an LUV sucrose density gradient flotation assay was performed comparing the ability of FκLCs to associate with PC lipid species that have different levels of saturation in their acyl tails. Briefly, LUVs were prepared in a 3:1:1 molar ratio of a PC lipid, POPS, and POPE in 10% sucrose PBS and incubated with FκLCs at 37˚C for 2 h to approximate physiological conditions. After incubation, the LUV/FκLC mixture was separated by centrifugation over a sucrose gradient, with the LUV fraction recovered at the 5–20% sucrose density interphase.

LUV fractions were subjected to analysis by SPR to detect the presence of membrane-bound FκLCs by reactivity with MDX1097 (Fig. 4*C*). Both sphingomyelin- and POPC-based LUVs bound FκLCs, as indicated by reactivity with the MDX1097-coated sensor chip (306 ± 0.3 and 363 ± 0.3 RUs, respectively). In contrast, LUVs consisting of the unsaturated PC species, DOPC, showed no binding above the FκLC alone negative control fraction (109 ± 2.1 and 125 ± 7.3 RUs, respectively; Fig. 4*C*). These results are consistent with the previous data and confirm a requirement for saturated PC lipid species, such as sphingomyelin, for the association of FκLCs with membranes. Moreover, based on MDX1097 binding, LUV-associated FκLCs were recognizable as KMA.

KMA expression is sphingomyelin dependent

Because the previous experiment indicated a role for saturated PC lipids, such as sphingomyelin, in the binding of FκLCs to cell membranes, we examined the sphingomyelin levels in KMA-positive and -negative cell lines. Total sphingomyelin was measured according to the methods set out by Hojjati and Jiang (21) and was expressed either as the amount per 10^7 cells or per milligram of protein. Cell lines were separated into high and low FκLC secretors as previously determined (Fig. 1*B*). Within each of these groups there was one KMA-positive cell line and one KMA-negative cell line. Sphingomyelin levels were significantly higher in the KMA-positive cells, irrespective of the FκLC secretion status. Thus, for the high FκLC secretors, the KMA-positive cell line JJN-3 expressed ~2-fold more sphingomyelin than its KMA-negative counterpart, NCI-H929. For the low FκLC secretors, ARH-77_100 KMA-positive cells expressed 25–50% more sphingomyelin than did ARH-77_neg cells (Fig. 5*A*, 5*B*). These results

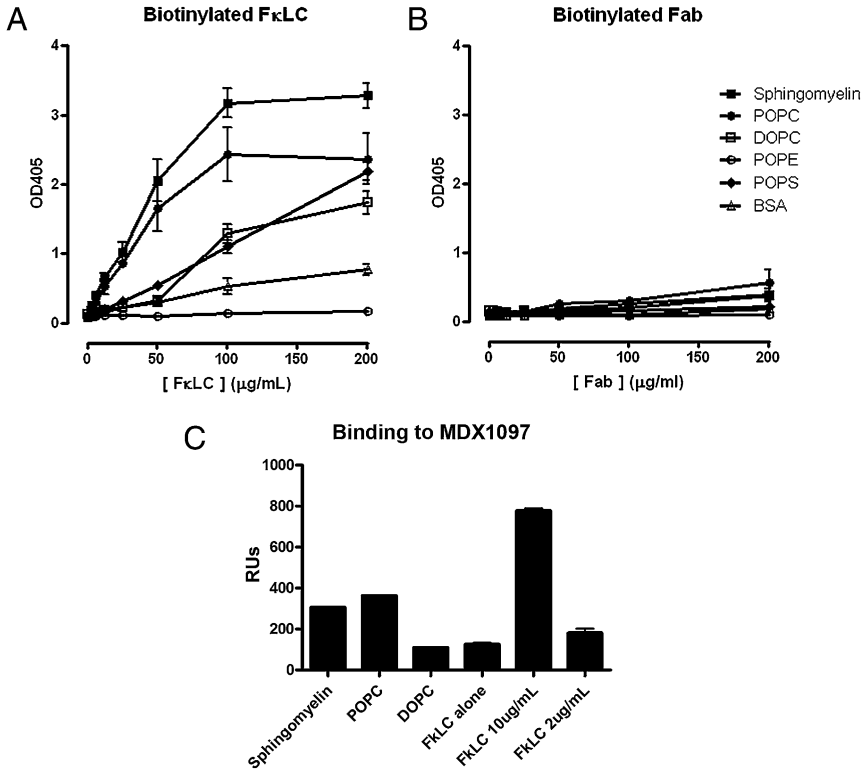

FIGURE 4. FκLCs bind saturated PC lipids and interact with cellular membranes. *A*, Phospholipid-coated microtiter wells were incubated with serial dilutions of biotinylated FκLC (*A*) or biotinylated Fab (*B*) and assessed for binding by detection with streptavidin-AP. *C*, SPR analysis of the binding of MDX1097 to LUVs composed of sphingomyelin, POPC, or DOPC and FκLCs. After incubation with FκLCs, LUVs were fractionated by sucrose density centrifugation and assessed for their ability to bind to an MDX1097-coated sensor chip. A BSA-coated chip was used as a control. Soluble FκLC standards at 10 and 2 μg/ml were used as positive controls. Data presented are means ± SE from two measurements.

show a clear positive correlation with respect to KMA expression and sphingomyelin levels.

Sphingomyelin levels were also assessed by the binding of lysenin, a protein with high specificity for sphingomyelin, to cell membranes (28, 29). KMA-positive (ARH-77_100 and JJN-3 cells) and -negative cell lines (ARH-77_neg and NCI-H929 cells) were incubated with biotinylated lysenin followed by staining with streptavidin-allophycocyanin. Cells were then analyzed by flow cytometry to measure the level of lysenin binding. Based on geometric mean fluorescence intensity, both of the KMA-positive cell lines expressed higher levels of plasma membrane sphingomyelin compared with the KMA-negative cells (Fig. 5*C*, 5*D*). Given the trend of increased plasma membrane sphingomyelin and KMA expression, these results further support the hypothesis that KMA is associated with sphingomyelin on the plasma membrane.

Neutral sphingomyelinase is an enzyme responsible for the breakdown of sphingomyelin into ceramide and PC (30). Disruption of this pathway by a highly specific small molecule neutral sphingomyelinase inhibitor (GW4869) results in the accumulation of sphingomyelin in cellular membranes (31). It was reasoned that if sphingomyelin was directly associated with KMA, then upregulation of the phospholipid by GW4869 would increase KMA expression in FκLC-secreting cells.

GW4869 treatment resulted in upregulation of sphingomyelin levels in all cell lines except ARH-77_100, and upregulation of sphingomyelin was highly correlated with KMA expression. KMA expression was increased in the KMA-positive cell line, JJN3, whereas the two KMA-negative cell lines, NCI-H929 and ARH-77_neg, were induced to express the Ag after treatment with GW4869. ARH-77_100 cells failed to upregulate plasma membrane sphingomyelin levels in response to GW4869, and, consistent with this, they did not express higher levels of KMA (Fig. 5*D*). The failure of ARH-77_100 to respond to GW4869 treatment may indicate that membrane sphingomyelin levels are saturated in these cells. Analysis of cell supernatants by SPR showed that FκLC secretion levels from all cell lines were actually lower after GW4869 treatment (data not shown). Because KMA upregulation could not be accounted for by an increase in FκLC secretion, these results, together with the lipid binding studies, clearly demonstrate that sphingomyelin is an important membrane component for the expression of KMA by FκLC-secreting cells.

The V domain is required for KMA expression

To gain further insight into the mechanism by which FκLCs bind to the plasma membrane, HEK-293 cells were transfected with genes encoding either the full-length JJN-3 κLC or a truncated form of JJN-3 κLC, encoding only the C domain. The latter construct retains the epitope bound by K-1-21 and MDX1097 (Supplemental Table 1) (9). Cells were harvested 3 d posttransfection and analyzed for KMA expression by flow cytometry. KMA expression was observed on the full-length κLC transfectants (8.7% KMA-positive cells) but was absent on the C domain only transfectants (Fig. 5*E*). Importantly, both tranfectants expressed comparable amounts of secreted product (1.0:0.9 molar ratio of normal κLCs/C domain only κLCs; Supplemental Table 1). These results clearly indicate that the V domain of FκLCs is necessary for stable association of the protein with the plasma membrane as KMA.

Identification of a putative binding site for PC in κLC V domains

Our experimental findings demonstrate that FκLC interacts with PC-saturated lipid species (Fig. 4), and that the interaction is dependent on the V domain (Fig. 5*E*). Thus, molecular docking was used to examine possible binding modes of the PC lipid head group into a conserved pocket identified in the V domains of κLCs (Fig. 6). Docking of the PC ligand demonstrates that it is primarily anchored to the binding site via interaction of the $N^{+}(CH_3)_3$ group (i.e., the charged portion of the choline moiety) with Asp^{82} and hydrogen bonding of the phosphate group with Lys^{39} (Fig. 6*A*). Close contacts also occur between the PC ligand and hydrophobic residues such as Phe^{62}. Although interactions are very similar

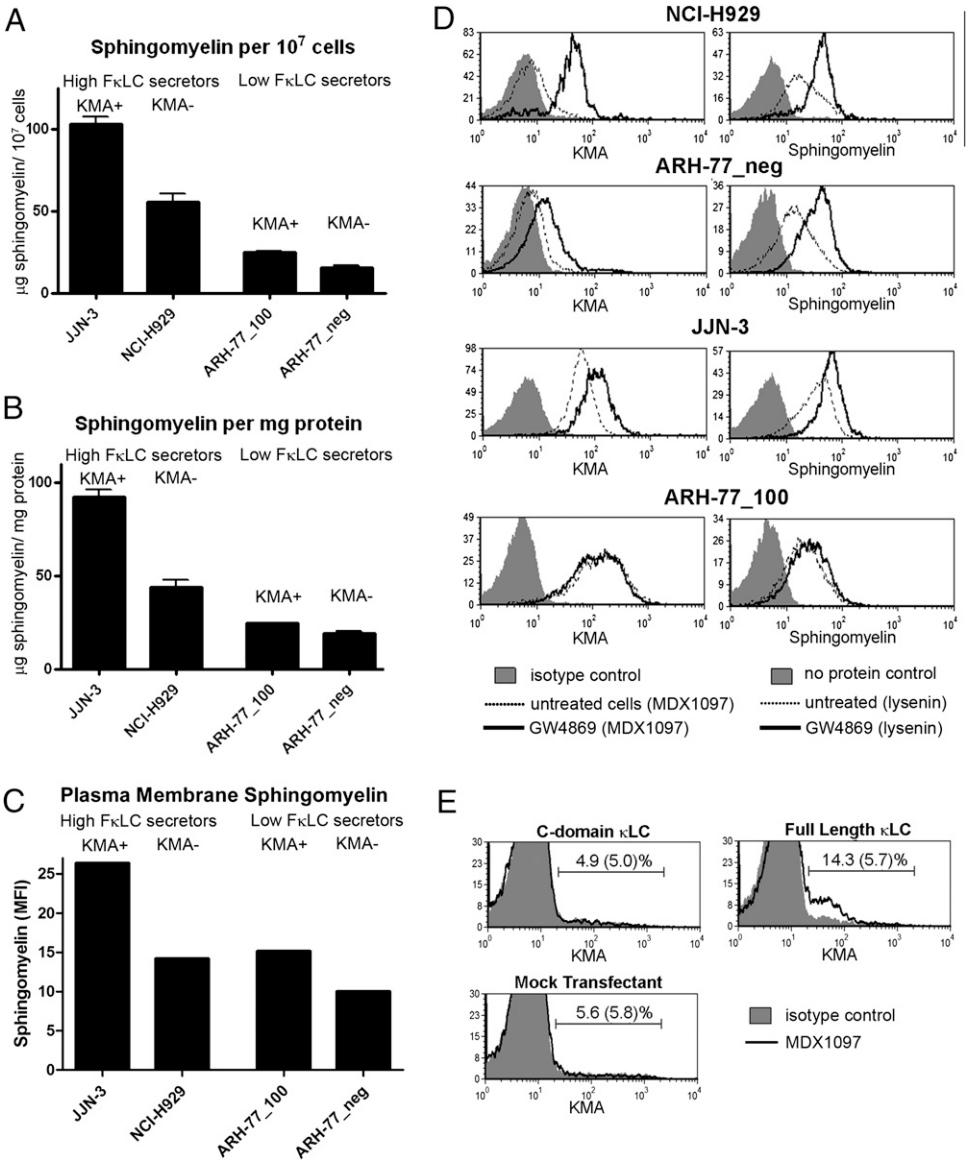

FIGURE 5. KMA expression is dependent on sphingomyelin and the V domain. Cell lines were grouped according to their level of FκLC secretion; that is, JJN-3 and NCI-H929 (high FκLC secretors) and ARH-77_100 and ARH-77_neg (low FκLC secretors) were assayed for total sphingomyelin. Total sphingomyelin was expressed per 10^7 cells (*A*) or per milligram of protein (*B*). Data presented are means ± SE from two measurements. *C*, Sphingomyelin-specific lysenin staining of cell lines assessed by flow cytometry and expressed as geometric mean fluorescence intensity above background control (values obtained from Fig. 5*D*). *D*, Flow cytometric analysis of sphingomyelin and KMA on cells incubated in the presence (solid black line) or absence (dotted black line) of 5 μM GW4869 for 48 h. Cells were then assessed for expression of KMA or sphingomyelin by flow cytometry. Solid gray histograms represent isotype control (for KMA staining) and no protein control (for sphingomyelin staining). *E*, Plasmids encoding JJN-3 full-length κLCs or C domain-only κLCs were transfected into HEK-293 cells. A mock transfection with no plasmid was used as a negative control. Flow cytometric analysis of KMA on HEK-293 cells transfected with genes encoding either the full-length JJN-3 κLCs or the C domain alone. Cells were stained 3 d posttransfection with either MDX1097 (black histogram) or human IgG isotype control (solid gray histogram). Mock-transfected cells were included as a negative control.

for the two binding sites of the κLC dimer, due to subtle conformational differences in the protein, the binding site on chain B provides an additional carboxylate group (Glu^{81}) for interaction with the choline moiety (Fig. 6*A*). A surface view shows that the putative PC binding cavity is of a suitable size for accommodating the ligand with the choline moiety binding by an end-on insertion mechanism (Fig. 6*B*), which is a typical binding mode for haptens and some small carbohydrates and peptides (32, 33). Importantly, the phosphate group is bound near the entrance to the cavity in a position suitable for extension with the lipid tail, that is, pieces representative of membrane lipids. Views of the two LC monomers show that the proposed binding of PC in the V domain is unimpeded by the conformation of the LC, being either extended or bent with respect to the positions of the V and C domains (Fig. 6C). Additionally, the binding of two PC ligands could easily occur in a FκLC dimer, as illustrated with the docked model shown in Fig. 6*D* (model derived from PDB structure 1B6D).

Discussion

Membrane extraction studies reveal that FκLCs are in direct association with the plasma membrane as KMA. This was confirmed in experiments that showed that FκLCs can bind directly to membranes composed of saturated PC lipids. Furthermore, heat-induced aggregation substantially increases binding of FκLCs to LUVs, suggesting that self-association is required for stable interaction with membranes. This was supported by BN-PAGE anal-

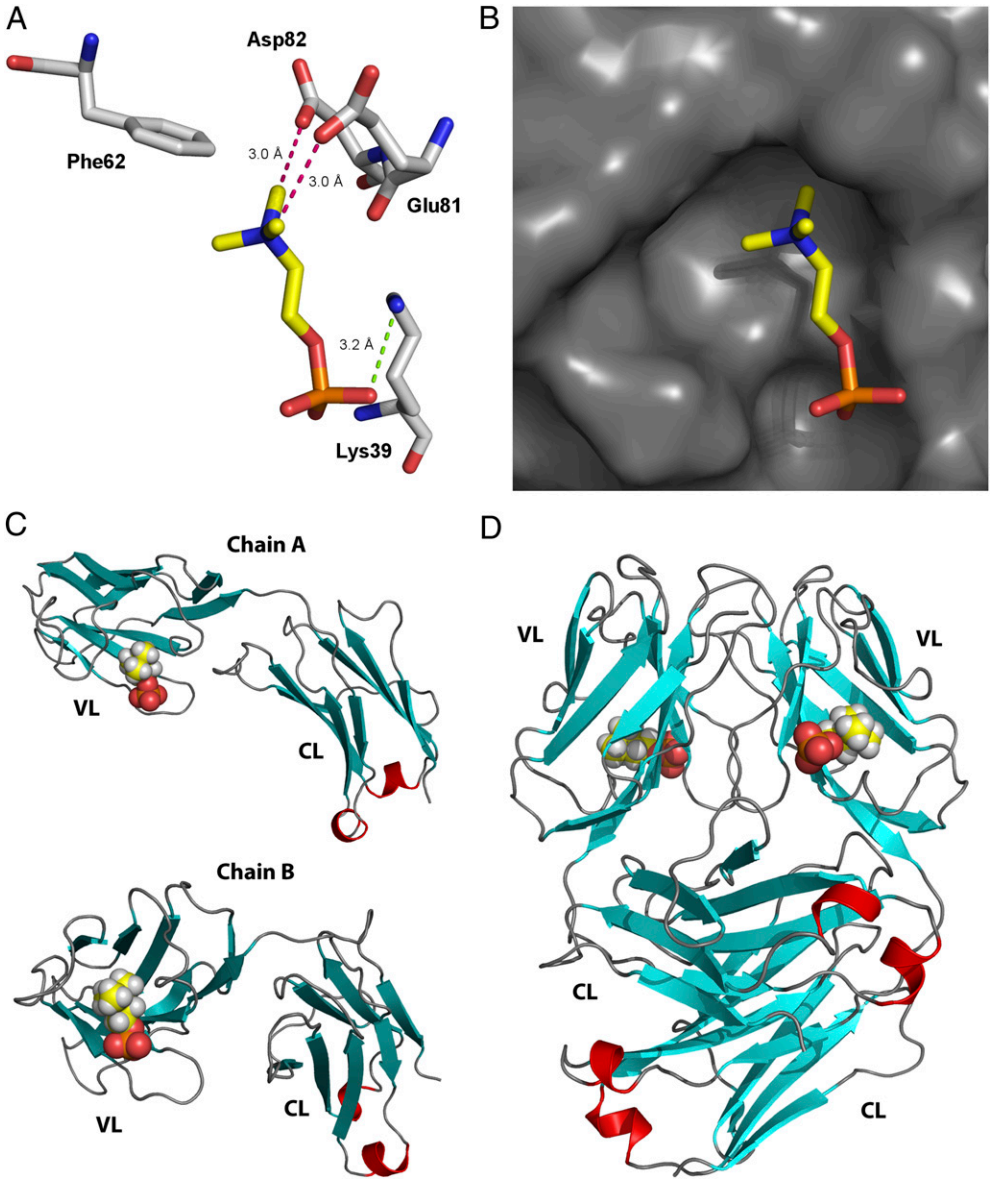

FIGURE 6. Molecular docking predicts a conserved PC binding site in the V domains of κLCs. *A*, Key interactions taking place in the top scoring pose of PC docked into the binding site on chain A/B of PDB code 1B6D. Atoms are colored by type (ligand C, yellow; protein C, white; N, blue; O, red; P, orange). Hydrogen bonds are shown as green dashed lines. Closest distances between the positively charged choline group and negatively charged amino acid side chains are shown as magenta dashed lines. *B*, Surface representation of chain A/B of 1B6D, with the top scoring pose of PC docked into the binding site. *C*, Ribbon representations of the A and B chains with the top scoring PC pose displayed as a space-filling model (van der Waals spheres). *D*, Ribbon representation of 1B6D with the top scoring poses of PC docked in the respective binding sites on the A and B chains. For ribbon representations, the protein is colored by secondary structure type (β sheet, cyan; α helix, red; loops and other conformations, gray). The ligand atoms are colored as for *A*, with methyl hydrogen atoms in white. CL, constant L chain domain; VL, variable L chain domain.

ysis of membrane proteins from ARH-77_100 cells, which showed that KMA resides in a large protein complex of ~480 kDa. Separation of this complex by SDS-PAGE under nonreducing conditions revealed the presence of FκLC monomers, indicating that KMA is composed of FκLC aggregates.

κLCs can also be found in association with HCs as part of the BCR on MM cells; however, KMA is clearly distinguishable from this complex. For example, K-1-21 and its human chimeric equivalent, MDX-1097, exhibit well-defined specificity for FκLCs and show no reactivity with HC-associated κLCs (10). When these mAbs are used to immunoprecipitate KMA from myeloma cell membranes, only FκLC is eluted, which indicates that KMA is not composed of HC-associated κLCs (Supplemental Fig. 1) (14). Furthermore, when solubilized plasma membranes from KMA-expressing cells are fractionated by SDS-PAGE under nonreducing conditions and probed with anti-κLCs, FκLCs are detected, whereas HC-associated κLCs in the form of Ig is not observed (Supplemental Fig. 2), indicating that Ig is either not present or is present at levels below the detection limit of the assay.

As FκLC is a secreted molecule, membrane association may occur on membranes of vesicles destined for exocytosis. This is supported by the finding that brefeldin A, which blocks the normal secretion route in eukaryotic cells, inhibits KMA expression on ARH-77_100 cells (see Supplemental Fig. 4). Our studies showed that FκLCs interact with mono- and disaturated PC lipid species, such as sphingomyelin and POPC, and that KMA expression can be induced on KMA-negative cell lines by increasing sphingomyelin levels. As such, these findings suggest that in high enough

concentrations of these lipids, FκLCs bind to membranes of vesicles that are destined for secretion and become exposed on the extracellular face as KMA during exocytosis. A schematic for KMA expression that accounts for our experimental findings is presented in Fig. 7.

An interesting aspect of the membrane extraction studies is that membrane-associated FκLCs, as KMA, share properties of both integral and peripheral-associated membrane proteins. In particular, KMA was found to be associated with the membrane via a combination of hydrophobic and electrostatic forces. Given the evidence that FκLCs are aggregated on the membrane, the electrostatic component observed in the membrane extraction study may represent the interaction of PC-charged head groups with individual FκLC molecules. The hydrophobic component, which is thought to govern aggregation processes (34, 35), may indicate interactions between adjacent FκLC molecules. In support of this model, the λ isotype of LCs was previously shown to interact directly with artificial membranes composed of POPC. This was a two-step process with an initial electrostatic interaction followed by a higher energy driven hydrophobic effect. The authors described this second event as a reorientation of Ig domains (36). In light of our findings with FκLCs, the binding of FκLCs could be interpreted as a self-association (aggregation) event after an initial contact with the membrane. Furthermore, this finding suggests that membrane association is a property of both LC isotypes. Subsequently, we have discovered the λLC equivalent to KMA, termed λ myeloma Ag (LMA), which is found on the surface of λ isotype MM cells (D.R. Jones, A.T. Hutchinson, P. Asvadi, R.D. Dunn, R.L. Raison, manuscript in preparation).

We also identified a highly conserved pocket in V domains of LCs that exhibited surface-exposed positive and negative charges that may interact with a zwitterionic PC molecule. Molecular docking studies showed that PC could be accommodated in this region via electrostatic and van der Waals forces between Asp^{82} and positively charged choline, hydrogen bonding of Lys^{39} with the phosphate group, and a hydrophobic interaction between choline and Phe^{62}. An additional carboxylate group (Glu^{81}) can interact with the choline moiety with only small adjustments in the putative PC binding cavity. Importantly, PC is orientated so that if acyl groups are present, as in a saturated lipid, then these could extend outward from the binding pocket as part of a membrane. Because this is a model, the interaction of PC with this region would need to be validated by experimental findings. Note, however, that in crystal structures of the λLC dimer, Mcg, heavy atom compounds bind (37), and zinc ions are likely to be found in this pocket (38), which supports its putative role in binding ligands such as PC.

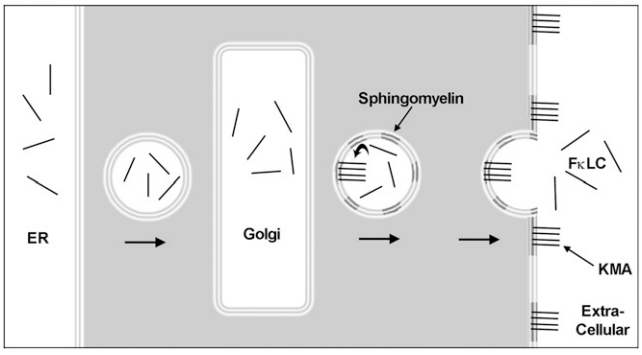

FIGURE 7. Model of KMA expression by a FκLC-secreting cell. FκLCs are synthesized in the ER and then transported to the Golgi apparatus. FκLCs are encapsulated into secretion vesicles. During transport to the plasma membrane, FκLCs associate and then aggregate on vesicular membranes composed of high levels of saturated PC lipids such as sphingomyelin. During exocytosis, fusion of the vesicle with the plasma membrane exposes membrane-associated FκLCs on the extracellular face as KMA. ER, endoplasmic reticulum.

Studies have suggested that membrane association is a general property shared by many aggregation-prone proteins (15, 39). In fact, it has been argued that amyloid formation in vivo actually arises due to specific interactions of proteins with lipid bilayers. One general model of amyloid deposition proposed that fibril formation arises via several distinct steps: 1) the initial protein–lipid interaction, which is thought to be electrostatic; 2) a conformational change in the protein that allows for self-association; 3) aggregation on the membrane surface; and 4) fibril formation as individual molecules grow outward from the membrane-associated aggregate (15). In relationship to our studies, membrane association may proceed in a similar manner whereby FκLCs undergo a conformational change after interaction with saturated PC lipids, allowing them to self-associate and stabilize on the membrane surface as KMA. It also follows that the process of aggregation in vivo by FκLCs, such as in LC amyloidosis and LC deposition disease, may be induced by saturated PC lipids present on membrane surfaces. Interestingly, a recent study by Farrugia et al. (40) showed that Fab molecules aggregate in the presence of zinc ions. Because the proposed PC binding site is structurally homologous to the zinc binding site in λLC (as previously discussed), it is possible that these ligands may induce aggregation by similar mechanisms.

FκLC is not unique in that α-synuclein, which is the primary structural component of Lewy body fibrils, has also been found to exist as a plasma membrane-associated aggregate on the neuronal cells that secrete the protein in its native form (16). This raises the question as to whether other aggregation-prone proteins can associate with the extracellular plasma membrane face in a similar fashion. In one study, insulin has been shown to directly associate with the plasma membrane of rat pancreatic cells, and this was dependent on the rates of secretion (41). With similarities to FκLC and α-synuclein, insulin can also undergo self-aggregation in the form of an amyloid (42, 43). As such, it would be interesting to ascertain whether insulin requires aggregation to associate with plasma membranes on islet cells.

In summary, we have described the characteristics required for a FκLC-secreting plasma cell to express KMA. We found that FκLC directly associates with saturated PC lipid species such as sphingomyelin. Moreover, increasing the levels of sphingomyelin in cell membranes was able to induce KMA expression in otherwise non-KMA–expressing cell lines. Although we cannot exclude a role for other PC-containing lipids, such as POPC, our data support a dominant role for sphingomyelin in the membrane association of FκLCs in the form of KMA. As membrane-associated FκLCs exist as large-molecular mass species, we propose that the interaction with these lipids causes FκLCs to self-associate into aggregates that are stabilized by multivalent binding on the membrane. It follows that exocytosis of the secretory vesicle allows for fusion with the plasma membrane exposing membrane-associated FκLCs on the extracellular face as KMA. It is well known that protein aggregates can bind membranes (15, 39). However, this is only the second example of protein aggregates being observed on the extracellular membrane surface of cells that are secreting the protein in its native form. Future work could explore whether other cells that secrete aggregation-prone proteins also express a plasma membrane-associated form of the molecule. This could lead to the development of compounds that specifically target the plasma membrane form of the protein and thereby help eliminate the cells responsible for the production of pathogenic protein aggregates.

Disclosures

A.T.H., D.R.J., M.E.L., C.V.J., and R.L.R. are previous employees of Immune System Therapeutics Ltd. A.B.E. has served in an advisory role to Immune System Therapeutics Ltd. A.T.H., D.R.J., C.V.J., A.B.E., and R.L.R. own stock in Immune System Therapeutics Ltd.

References

1. Kyle, R. A., and S. V. Rajkumar. 2008. Multiple myeloma. *Blood* 111: 2962–2972.
2. Merlini, G., and V. Bellotti. 2003. Molecular mechanisms of amyloidosis. *N. Engl. J. Med.* 349: 583–596.
3. Sikkink, L. A., and M. Ramirez-Alvarado. 2008. Biochemical and aggregation analysis of Bence Jones proteins from different light chain diseases. *Amyloid* 15: 29–39.
4. Qin, Z., D. Hu, M. Zhu, and A. L. Fink. 2007. Structural characterization of the partially folded intermediates of an immunoglobulin light chain leading to amyloid fibrillation and amorphous aggregation. *Biochemistry* 46: 3521–3531.
5. Khurana, R., J. R. Gillespie, A. Talapatra, L. J. Minert, C. Ionescu-Zanetti, I. Millett, and A. L. Fink. 2001. Partially folded intermediates as critical precursors of light chain amyloid fibrils and amorphous aggregates. *Biochemistry* 40: 3525–3535.
6. Helms, L. R., and R. Wetzel. 1996. Specificity of abnormal assembly in immunoglobulin light chain deposition disease and amyloidosis. *J. Mol. Biol.* 257: 77–86.
7. Meng, X., A. L. Fink, and V. N. Uversky. 2008. The effect of membranes on the in vitro fibrillation of an amyloidogenic light-chain variable-domain SMA. *J. Mol. Biol.* 381: 989–999.
8. Rajkumar, S. V., R. A. Kyle, T. M. Therneau, R. J. Clark, A. R. Bradwell, L. J. Melton, III, D. R. Larson, M. F. Plevak, and J. A. Katzmann. 2004. Presence of monoclonal free light chains in the serum predicts risk of progression in monoclonal gammopathy of undetermined significance. *Br. J. Haematol.* 127: 308–310.
9. Raison, R. L., and H. A. Boux. 1985. Conformation dependence of a monoclonal antibody defined epitope on free human kappa chains. *Mol. Immunol.* 22: 1393–1398.
10. Boux, H. A., R. L. Raison, K. Z. Walker, G. E. Hayden, and A. Basten. 1983. A tumor-associated antigen specific for human κ myeloma cells. *J. Exp. Med.* 158: 1769–1774.
11. Boux, H. A., R. L. Raison, K. Z. Walker, E. Musgrove, and A. Basten. 1984. The surface expression of a tumor-associated antigen on human κ myeloma cells. *Eur. J. Immunol.* 14: 216–222.
12. Walker, K. Z., H. A. Boux, G. E. Hayden, C. C. Goodnow, and R. L. Raison. 1985. A monoclonal antibody with selectivity for human κ myeloma and lymphoma cells which has potential as a therapeutic agent. *Adv. Exp. Med. Biol.* 186: 833–841.
13. Spencer, A., P. Walker, P. Asvadi, M. Wong, D. Campbell, K. Reed, M. Copeman, G. Nichol, L. J. Cohen, and R. Dunn. 2010. A phase I study of the anti-κ monoclonal antibody, MDX-1097, in previously treated multiple myeloma patients. *J. Clin. Oncol.* 28: S15 (Abstr. 8143).
14. Goodnow, C. C., and R. L. Raison. 1985. Structural analysis of the myeloma-associated membrane antigen KMA. *J. Immunol.* 135: 1276–1280.
15. Gorbenko, G. P., and P. K. J. Kinnunen. 2006. The role of lipid-protein interactions in amyloid-type protein fibril formation. *Chem. Phys. Lipids* 141: 72–82.
16. Dixon, C., N. Mathias, R. M. Zweig, D. A. Davis, and D. S. Gross. 2005. α-Synuclein targets the plasma membrane via the secretory pathway and induces toxicity in yeast. *Genetics* 170: 47–59.
17. Schweizer, A., O. Valdenaire, P. Nelböck, U. Deuschle, J. B. Dumas Milne Edwards, J. G. Stumpf, and B. M. Löffler. 1997. Human endothelin-converting enzyme (ECE-1): three isoforms with distinct subcellular localizations. *Biochem. J.* 328: 871–877.
18. Fujiki, Y., A. L. Hubbard, S. Fowler, and P. B. Lazarow. 1982. Isolation of intracellular membranes by means of sodium carbonate treatment: application to endoplasmic reticulum. *J. Cell Biol.* 93: 97–102.
19. Koppel, D. E. 1972. Analysis of macromolecular polydispersity in intensity correlation spectroscopy: the method of cumulants. *J. Chem. Phys.* 57: 4814–4821.
20. Hope, M. J., M. B. Bally, G. Webb, and P. R. Cullis. 1985. Production of large unilamellar vesicles by a rapid extrusion procedure: characterization of size distribution, trapped volume and ability to maintain a membrane potential. *Biochim. Biophys. Acta* 812: 55–65.
21. Hojjati, M. R., and X. C. Jiang. 2006. Rapid, specific, and sensitive measurements of plasma sphingomyelin and phosphatidylcholine. *J. Lipid Res.* 47: 673–676.
22. Roussel, A., S. Spinelli, S. Déret, J. Navaza, P. Aucouturier, and C. Cambillau. 1999. The structure of an entire noncovalent immunoglobulin κ light-chain dimer (Bence-Jones protein) reveals a weak and unusual constant domains association. *Eur. J. Biochem.* 260: 192–199.
23. Hutt, D. M., L. F. Da-Silva, L. H. Chang, D. C. Prosser, and J. K. Ngsee. 2000. PRA1 inhibits the extraction of membrane-bound Rab GTPase by GDI1. *J. Biol. Chem.* 275: 18511–18519.
24. David, V., F. Hochstenbach, S. Rajagopalan, and M. B. Brenner. 1993. Interaction with newly synthesized and retained proteins in the endoplasmic reticulum suggests a chaperone function for human integral membrane protein IP90 (calnexin). *J. Biol. Chem.* 268: 9585–9592.
25. Boonsirichai, K., J. C. Sedbrook, R. Chen, S. Gilroy, and P. H. Masson. 2003. Altered Response to Gravity is a peripheral membrane protein that modulates gravity-induced cytoplasmic alkalinization and lateral auxin transport in plant statocytes. *Plant Cell* 15: 2612–2625.
26. Drenan, R. M., X. Liu, P. G. Bertram, and X. F. Zheng. 2004. FKBP12-rapamycin-associated protein or mammalian target of rapamycin (FRAP/mTOR) localization in the endoplasmic reticulum and the Golgi apparatus. *J. Biol. Chem.* 279: 772–778.
27. Vallas, V., W. Farrugia, R. L. Raison, A. B. Edmundson, and P. A. Ramsland. 2007. Dissimilar aggregation processes govern precipitation and gelation of human IgM cryoglobulins. *J. Mol. Recognit.* 20: 90–96.
28. Yamaji, A., Y. Sekizawa, K. Emoto, H. Sakuraba, K. Inoue, H. Kobayashi, and M. Umeda. 1998. Lysenin, a novel sphingomyelin-specific binding protein. *J. Biol. Chem.* 273: 5300–5306.
29. Shakor, A. B. A., E. A. Czurylo, and A. Sobota. 2003. Lysenin, a unique sphingomyelin-binding protein. *FEBS Lett.* 542: 1–6.
30. Tomiuk, S., K. Hofmann, M. Nix, M. Zumbansen, and W. Stoffel. 1998. Cloned mammalian neutral sphingomyelinase: functions in sphingolipid signaling? *Proc. Natl. Acad. Sci. USA* 95: 3638–3643.
31. Luberto, C., D. F. Hassler, P. Signorelli, Y. Okamoto, H. Sawai, E. Boros, D. J. Hazen-Martin, L. M. Obeid, Y. A. Hannun, and G. K. Smith. 2002. Inhibition of tumor necrosis factor-induced cell death in MCF7 by a novel inhibitor of neutral sphingomyelinase. *J. Biol. Chem.* 277: 41128–41139.
32. Ramsland, P. A., W. Farrugia, E. Yuriev, A. B. Edmundson, and M. S. Sandrin. 2003. Evidence for structurally conserved recognition of the major carbohydrate xenoantigen by natural antibodies. *Cell. Mol. Biol. (Noisy-le-grand)* 49: 307–317.
33. Ramsland, P. A., E. Yuriev, and A. B. Edmundson. 2001. Immunoglobulin cross-reactivity examined by library screening, crystallography and docking studies. *Comb. Chem. High Throughput Screen.* 4: 397–408.
34. Jaenicke, R. 1995. Folding and association versus misfolding and aggregation of proteins. *Philos. Trans. R. Soc. Lond. B Biol. Sci.* 348: 97–105.
35. Goloubinoff, P., and A. P. Ben-Zvi. 2006. Mechanisms of active solubilization of stable protein aggregates by molecular chaperones. In *Protein Misfolding, Aggregation and Conformational Diseases: Part A: Protein Aggregation and Conformational Diseases.* V. N. Uversky, and A. L. Fink, eds. Springer, New York, p. 165–174.
36. Wall, J. S., F. M. Ayoub, and P. S. O'Shea. 1996. A study of the interactions of an immunoglobulin light chain with artificial and B-lymphocyte membranes. *Front. Biosci.* 1: a46–a58.
37. Schiffer, M., R. L. Girling, K. R. Ely, and A. B. Edmundson. 1973. Structure of a λ-type Bence-Jones protein at 3.5-Å resolution. *Biochemistry* 12: 4620–4631.
38. Hanson, B. L., G. J. Bunick, J. M. Harp, and A. B. Edmundson. 2002. Mcg in 2030: new techniques for atomic position determination of immune complexes. *J. Mol. Recognit.* 15: 297–305.
39. Fernández, A., and R. S. Berry. 2003. Proteins with H-bond packing defects are highly interactive with lipid bilayers: implications for amyloidogenesis. *Proc. Natl. Acad. Sci. USA* 100: 2391–2396.
40. Farrugia, W., A. M. Scott, and P. A. Ramsland. 2009. A possible role for metallic ions in the carbohydrate cluster recognition displayed by a Lewis Y specific antibody. *PLoS ONE* 4: e7777.
41. Kaplan, D. R., J. R. Colca, and M. L. McDaniel. 1983. Insulin as a surface marker on isolated cells from rat pancreatic islets. *J. Cell Biol.* 97: 433–437.
42. Jiménez, J. L., E. J. Nettleton, M. Bouchard, C. V. Robinson, C. M. Dobson, and H. R. Saibil. 2002. The protofilament structure of insulin amyloid fibrils. *Proc. Natl. Acad. Sci. USA* 99: 9196–9201.
43. Hua, Q. X., and M. A. Weiss. 2004. Mechanism of insulin fibrillation: the structure of insulin under amyloidogenic conditions resembles a protein-folding intermediate. *J. Biol. Chem.* 279: 21449–21460.